Available at www.sciencedirect.com

ScienceDirect

journal homepage: www.elsevier.com/locate/he

A two-stage hydrogen compressor based on (La,Ce,Nd,Pr) Ni_5 intermetallics obtained by low energy mechanical alloying – Low temperature annealing treatment

B.A. Talagañis[a,b], M.R. Esquivel[a,b,c,d,*], G. Meyer[a,b,c]

[a]Instituto Balseiro (UNCu and CNEA), Centro Atómico Bariloche, Av. Bustillo km 9.5 (R8402AGP), S.C. de Bariloche, Argentina
[b]Consejo Nacional de Investigaciones Científicas y Técnicas, Argentina
[c]Comisión Nacional de Energía Atómica, Centro Atómico Bariloche, Av. Bustillo km 9.5 (R8402AGP), S.C. de Bariloche, Argentina
[d]Centro Regional Universitario Bariloche (UNCo), Quintral 1250 (R8400FRF), S.C. de Bariloche, Argentina

ARTICLE INFO

Article history:
Received 5 October 2008
Received in revised form
21 November 2008
Accepted 21 November 2008
Available online 21 January 2009

Keywords:
AB_5
(La,Ce)Ni_5
Mechanical alloying
Hydrogen compression

ABSTRACT

$La_{0.67}Ce_{0.19}Nd_{0.08}Pr_{0.06}Ni_5$ was synthesized by low energy mechanical alloying. The AB_5 was milled up to *completion stage* to reach the final composition and appropriate particle size distribution and microstructure characteristics. Crystallite size, strain and sorption properties of as-milled samples were evaluated. After milling, $La_{0.67}Ce_{0.19}Nd_{0.08}Pr_{0.06}Ni_5$ and previously obtained $LaNi_5$ were annealed at 600 °C for 24 h. An improvement in both microstructural and hydrogen sorption properties was found. Equilibrium hydrogen sorption properties were obtained and quantified in the 25–90 °C range. From these results, a two-stage hydrogen compressor was proposed. In the first stage, hydrogen is absorbed by $LaNi_5$ at 575 kPa and 25 °C and desorbed at 1365 kPa and 90 °C. In the second stage, this fluid is absorbed by $La_{0.67}Ce_{0.19}Nd_{0.08}Pr_{0.06}Ni_5$ at 745 kPa and 25 °C and desorbed at 2100 kPa and 90 °C. As a result, a global compression ratio of 3.65 is reached using this scheme.

1. Introduction

After the discovery of the hydrides of AB_5's [1], an important area of research was focused on the study of the engineering applications of these compounds [2]. Because of their thermodynamic properties, the thermal compression of hydrogen was identified as immediate technological application [2]. Two families of intermetallics were found to be suitable for this goal: AB_2's and AB_5's [3]. Research works on this subject were previously presented [4–8]. Industrial applications are currently used [9]. But the intermetallics used were synthesized by high temperature equilibrium methods [4–8]. As technology progressed, new synthesis methods of intermetallics replaced the traditional ones and mechanical alloying (MA) was used to synthesize AB_5 [10]. Nevertheless, straightforward application of materials obtained by this method is not possible. Material inhomogeneities and microstructure need to be improved before use in these devices [10–13]. But any after-milling treatment should be as short, economic and easy to apply as possible in order to facilitate the immediate application to hydrogen compression devices.

In this work, an integral treatment including synthesis by mechanical alloying and after-milling treatments was

* *Corresponding author*. Centro Atómico Bariloche – Comisión Nacional de Energía Atómica – Avda. Bustillo km 9,5 – Bariloche – Río Negro – (R8402AGP), Argentina. Tel.: +54 02944 445156; fax: +54 02944 445299.
E-mail address: esquivel@cab.cnea.gov.ar (M.R. Esquivel).
0360-3199/$ – see front matter © 2008 International Association for Hydrogen Energy. Published by Elsevier Ltd. All rights reserved.
doi:10.1016/j.ijhydene.2008.11.052

developed for AB_5-based intermetallics. Two different paths of synthesis were selected:

Low energy mechanical alloying of a mixture of metals according to:

$$La + 5Ni \rightarrow LaNi_5$$

Low energy mechanical alloying of a mixture of intermetallics according to:

$$LaNi_5 + MmNi_5\ [11,12] \rightarrow La_{0.67}Ce_{0.19}Nd_{0.08}Pr_{0.06}Ni_5$$

These compositions were selected to obtain a hydrogen compressor with both stages containing either binary or pseudo-binary intermetallics with low temperature absorption process at pressures lower than 1000 kPa and high temperature desorption at pressures lower than 2500 kPa [3,10]. The obtained materials were used in the design of a two-stage hydrogen thermal compressor reaching a compression ratio of 3.65.

This research work is integrated within the framework of a scientific and technical project oriented to the development of a hydrogen supply system for transport devices. These results are applied to the development of a multistage thermal compressor of hydrogen. This objective aimed the elaboration of the present work.

2. Experimental

$La_{0.67}Ce_{0.19}Nd_{0.08}Pr_{0.06}Ni_5$ ($MmNi_5$) was synthesized by low energy mechanical alloying (MA) in a Uni-Ball-Mill II apparatus (Australian Scientific Instruments) from $LaNi_5$ (pieces, 99.9%, Sigma–Aldrich) and $MmNi_5$ powder. $MmNi_5$ powder was previously synthesized by mechanical alloying from Pure Ni (99.99%, Sigma–Aldrich) and drilled lumps of Mischmetal (Mm) (99.7%, Alpha Aesar) of nominal composition 52.1 wt% Ce, 25.5 wt% La, 16.9 wt% Pr, 5.5 wt% Nd. Neutron Activation Analysis (NAA) and Energy Dispersive Spectroscopy (EDS) were used to verify Mm chemical composition. $MmNi_5$ synthesis features are detailed elsewhere [11,12]. $La_{0.67}Ce_{0.19}Nd_{0.08}Pr_{0.06}Ni_5$ synthesis was achieved under Ar atmosphere. The ball-to-powder mass relation selected was

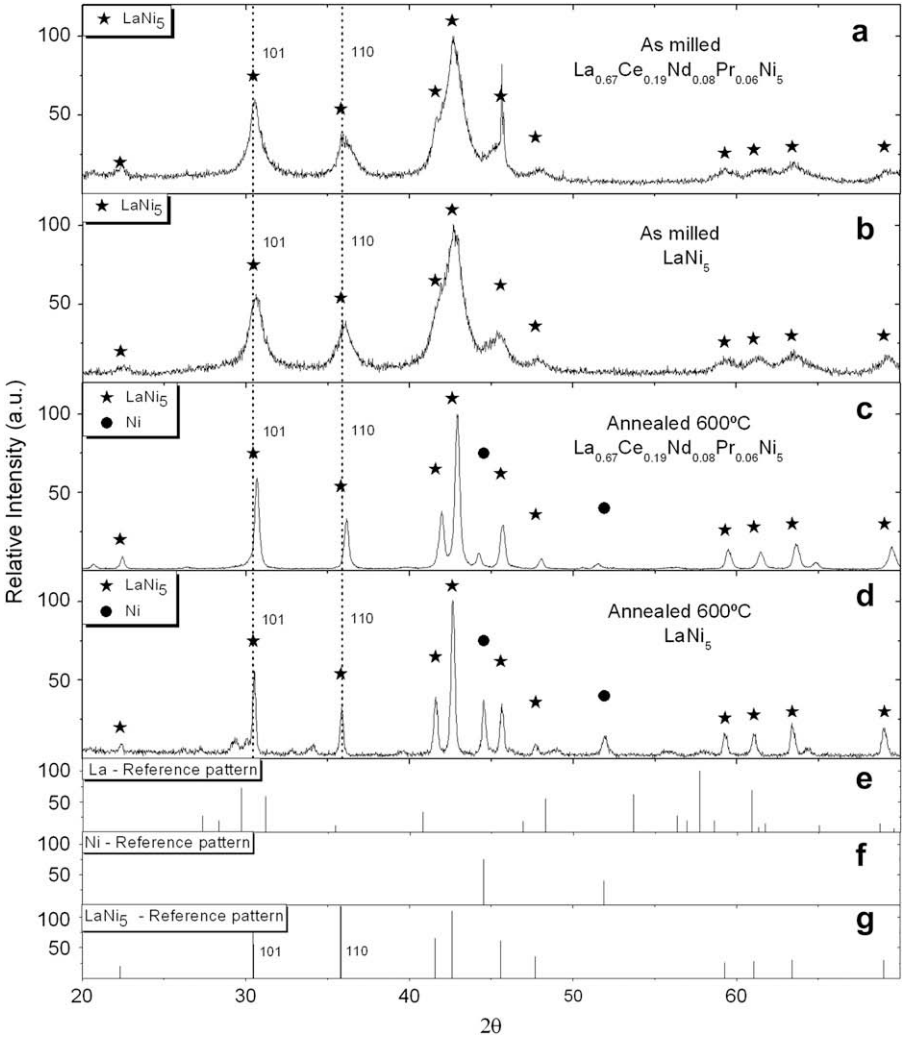

Fig. 1 – Diffractograms of AB_5's mechanically alloyed in a low energy mill, as-milled and milled + annealed at 600 °C for 24 h.

Table 1 – Crystallite size and strain changes due to milling and annealing.

Sample	Treatment	hkl	Crystallite size (Å) ± 10	Strain (%) ± 0.05
$LaNi_5$	As-milled (457 h)	101	200	1.35
		110	200	1.15
	Milled + annealed	101	1730	0.25
	600 °C	110	1730	0.20
$La_{0.67}Ce_{0.19}Nd_{0.08}Pr_{0.06}Ni_5$	As-milled (100 h)	101	220	1.20
		110	170	1.30
	Milled + annealed	101	750	0.45
	600 °C	110	830	0.35

22.5:1. Sample handling features are referenced elsewhere [11,12].

Room temperature X-ray diffraction was achieved on a Philips PW 1710/01 Instrument with Cu Kα radiation (graphite monocromator). Diffraction patterns were analyzed by the Rietveld method using DBWS software [14]. Particles size and morphology were observed by Scanning Electron Microscopy (SEM). Strain and crystallite size effects were estimated from diffraction peaks by assuming empirically a Gauss distribution and a Cauchy (Lorentz) component, respectively [15]. Chemical composition was verified by Energy Dispersive Spectroscopy (EDS) analysis. The enhancement of properties consisted in after-milling isothermal annealing at different temperatures (400 and 600 °C) for 24 h under pressures lower than 1×10^{-4} kPa.

Fully automatic Sieverts type equipment was used to measure hydrogen absorption-desorption features. The experimental set-up device is described elsewhere [16].

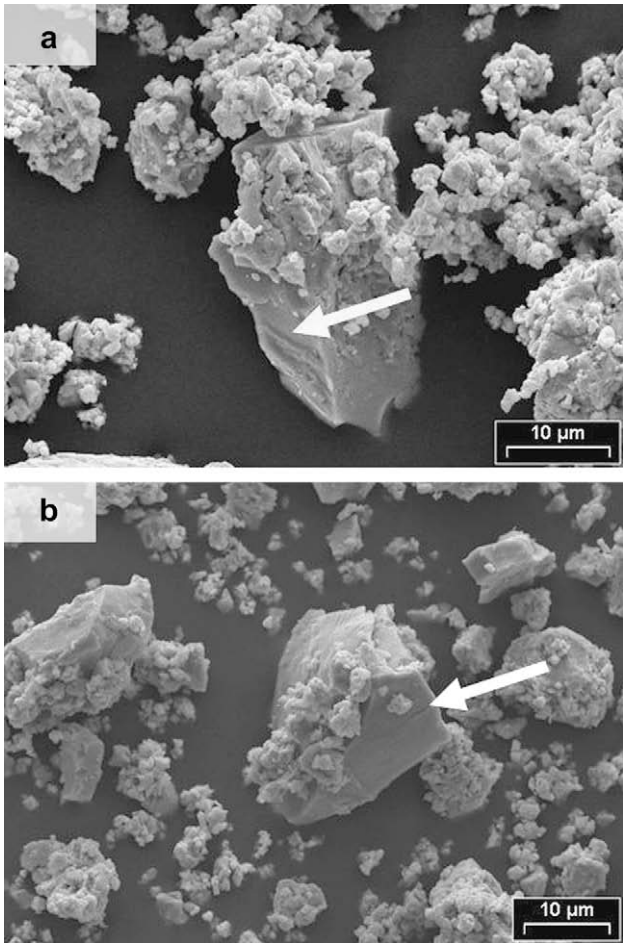

Fig. 2 – SEM images. a) Mechanically alloyed $LaNi_5$. b) Mechanically alloyed $La_{0.67}Ce_{0.19}Nd_{0.08}Pr_{0.06}Ni_5$.

Table 2 – Elemental composition of the $La_{0.67}Ce_{0.19}Nd_{0.08}Pr_{0.06}Ni_5$ sample. A and B sites elemental compositions are individually shown.

Sample	Particle size (μm × μm)	Elemental composition %				
		A*				B*
		La	Ce	Nd	Pr	Ni
$La_{0.67}Ce_{0.19}Nd_{0.08}Pr_{0.06}Ni_5$	10 × 10	68	18	8	6	100
	5 × 5	69	17	8	6	100
	10 × 5	68	18	8	6	100
	10 × 10	68	18	8	6	100
	7 × 10	68	18	8	6	100
	6 × 10	69	17	8	6	100

* indicates that A and B sites elemental composition are individually shown.

3. Results and discussion

3.1. Synthesis of $La_{0.67}Ce_{0.19}Nd_{0.08}Pr_{0.06}Ni_5$

The $LaNi_5$–$MmNi_5$ mixture was milled during 100 h under Ar atmosphere in order to synthesize $La_{0.67}Ce_{0.19}Nd_{0.08}Pr_{0.06}Ni_5$. The X-ray diffraction profile of the as-milled product is shown in Fig. 1a. Typical effects of milling, broad peaks and incipient amorphization, are observed. As-milled $LaNi_5$ obtained from a La–Ni mixture is also shown in Fig. 1b. Synthesis details of this intermetallic are presented elsewhere [17]. Reference pattern of $LaNi_5$ [18] is also presented in Fig. 1g for comparison.

But materials synthesized by mechanical alloying need a thermal treatment after milling in order to release strain and thereafter to improve hydrogen sorption properties [10,17]. The XRD profile after annealing the sample at 600 °C for 24 h is displayed in Fig. 1c. A well defined diffraction profile with thin peaks is observed in this figure. This thermal treatment

Table 3 – Comparison of the cell parameters values of the previously obtained $LaNi_5$ [17] with those of $La_{0.67}Ce_{0.19}Nd_{0.08}Pr_{0.06}Ni_5$. Wt% values of the AB_5 and Ni are shown. R_{wp} stands for the goodness of the Rietveld refinement.

Sample	a (Å)	c (Å)	V (Å^3)	Relative content wt%		R_{wp} (%)
				AB_5	Ni	
$LaNi_5$	5.013	3.976	86.53	85 ± 2	15 ± 1	10
$La_{0.67}Ce_{0.19}Nd_{0.08}Pr_{0.06}Ni_5$	4.975	3.976	85.22	95 ± 2	5 ± 1	12

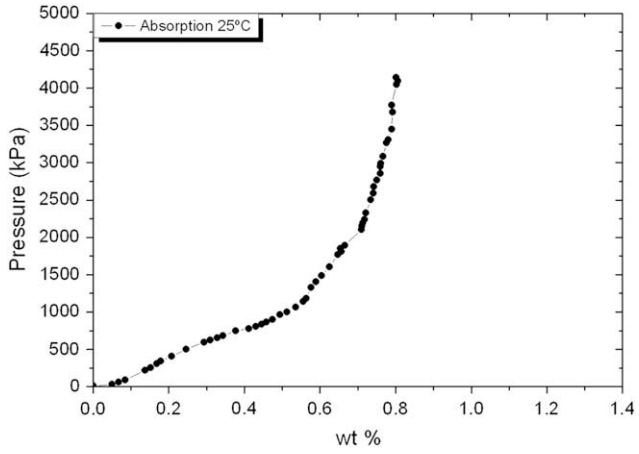

Fig. 3 – PCI of as-milled $La_{0.67}Ce_{0.19}Nd_{0.08}Pr_{0.06}Ni_5$.

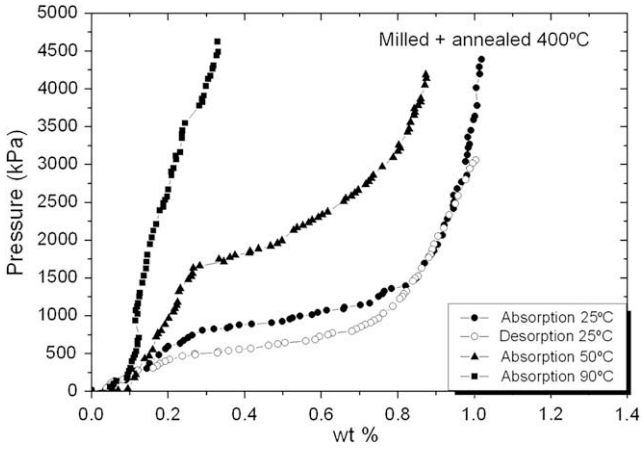

Fig. 4 – PCI's of $La_{0.67}Ce_{0.19}Nd_{0.08}Pr_{0.06}Ni_5$ (milled + annealed 400 °C for 24 h) at different temperatures.

assures the recrystallization for samples milled up to *completion stage* in this type of mill [11,12,17]. The same treatment was done for $LaNi_5$ as observed in Fig. 1d [17]. In each case, the peaks corresponding to both AB_5 and Ni phases are present, the only ones that occurs in the Ni-rich side of La–Ni and their related phase diagrams [19]. For comparison, La [20] and Ni [21] reference patterns are also shown in Fig. 1e and f. The presence of La_2O_3-based hydroxides and oxide-hydroxides is also observed [22,23]. These compounds occur from La_2O_3-based oxides formed previous to mechanical alloying, during Mm cleaning pre-treatment [11] and during exposure to ambient conditions while XRD collection data was taken. To quantify the microstructural changes due to annealing, crystallite size and strain were calculated for (101) and (110) hkl directions from X-ray profiles of Fig. 1a and c. For comparison, the same calculation was done for $LaNi_5$ presented in Fig. 1b and Fig. 1d [17]. A summary of results is shown in Table 1. The similarities in crystallite size and strain between both as-milled intermetallics indicates that *completion stage* [11,12,17] is reached at 100 h of integrated milling time. This assumption can also be confirmed by comparing the SEM images of Fig. 2. Both as-milled $LaNi_5$ (Fig. 2a) and $La_{0.67}Ce_{0.19}Nd_{0.08}Pr_{0.06}Ni_5$ (Fig. 2b) presents well faceted edges, typical of fragile fracture, and residual effects of cold welding. These last ones are indicated with arrows in the figures. In each case, particle size distribution was analyzed leading to a final average particle distribution size of 6 ± 3 μm and <6 μm for $La_{0.67}Ce_{0.19}Nd_{0.08}Pr_{0.06}Ni_5$ and $LaNi_5$, respectively.

EDS microanalysis was performed on sample $La_{0.67}Ce_{0.19}Nd_{0.08}Pr_{0.06}Ni_5$ to verify chemical composition. Results are summarized in Table 2.

Cell parameters were calculated from the XRD profiles of Fig. 1c and d. Values are presented in Table 3. A decrease in the cell volume of $La_{0.67}Ce_{0.19}Nd_{0.08}Pr_{0.06}Ni_5$ in comparison with that of $LaNi_5$ is observed. It is due to the change of the *a* parameter since the *c* one is almost constant. It affects

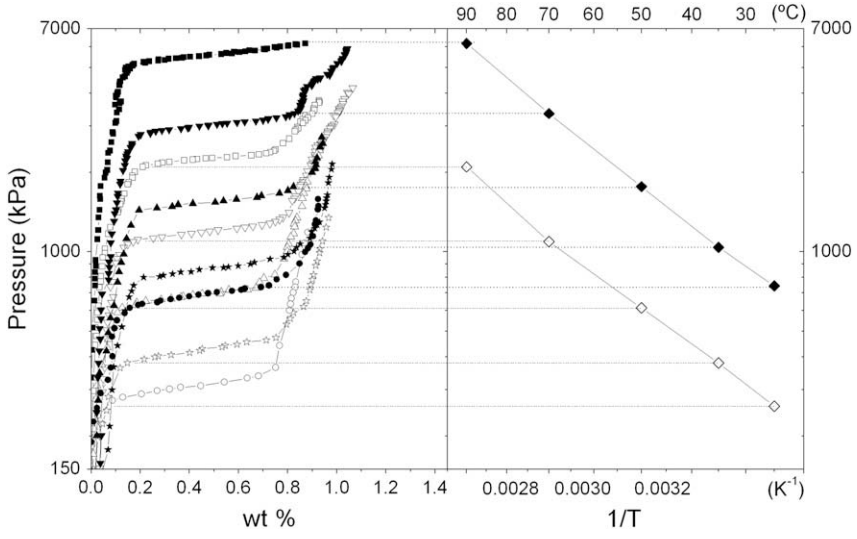

Fig. 5 – Left: PCI of $La_{0.67}Ce_{0.19}Nd_{0.08}Pr_{0.06}Ni_5$ (milled + annealed 600 °C) at 25●, 35★, 50▲, 70▼ and 90 °C■. Full symbols correspond to absorption, hollow symbols to desorption. Right: corresponding Van't Hoff diagram.

Table 4 – Hydriding properties of $LaNi_5$ [17] and $La_{0.67}Ce_{0.19}Nd_{0.08}Pr_{0.06}Ni_5$.

Sample	Treatment	Temperature (°C)	Pa range (kPa)	Pd range (kPa)	Capacity (wt%)	Hysteresis log (Pa/Pd)
$LaNi_5$	Milled + annealed 600 °C	25	393–577	237–175	1.26	0.37
		35	590–804	346–273	1.31	0.35
		50	966–1321	572–441	1.21	0.35
		70	1752–2213	1176–859	1.17	0.29
		90	3062–3679	2201–1366	1.07	0.28
$La_{0.67}Ce_{0.19}Nd_{0.08}Pr_{0.06}Ni_5$	Milled + annealed 400 °C	25	807–1500	772–465	0.55	0.27
		50	1660–2970	–	0.40	–
		90	–	–	–	–
$La_{0.67}Ce_{0.19}Nd_{0.08}Pr_{0.06}Ni_5$	Milled + annealed 600 °C	25	550–743	364–260	0.77	0.32
		35	746–1039	473–379	0.78	0.32
		50	1438–1767	794–613	0.77	0.36
		70	2744–3342	1407–1093	0.79	0.39
		90	5119–6161	2447–2099	0.73	0.39

directly the sorption properties of the intermetallic [24,25]. Quantification of $LaNi_5$-Ni and $La_{0.67}Ce_{0.19}Nd_{0.08}Pr_{0.06}Ni_5$-Ni mass percentages was performed by Rietveld method. Results are summarized in Table 3. In this table, R_{wp} stands for the goodness of the fit.

3.2. $La_{0.67}Ce_{0.19}Nd_{0.08}Pr_{0.06}Ni_5$ hydriding properties – as-milled

A pressure–composition isotherm (PCI) at 25 °C corresponding to as-milled $La_{0.67}Ce_{0.19}Nd_{0.08}Pr_{0.06}Ni_5$ is shown in Fig. 3. As observed, the non-annealed intermetallic presents a steeped plateau slope and half of the theoretical storage capacity. This behavior is explained by the microstructural inhomogeneities present in the sample. Under these conditions, the intermetallic is not suitable for the operation of a stable and efficient hydrogen compression stage.

3.3. $La_{0.67}Ce_{0.19}Nd_{0.08}Pr_{0.06}Ni_5$ hydriding properties – after thermal treatment

A post milling annealing treatment is necessary to improve the intermetallic hydriding properties [10,17]. As-milled $La_{0.67}Ce_{0.19}Nd_{0.08}Pr_{0.06}Ni_5$ was annealed for 24 h at 400 and 600 °C. After each treatment, hydrogen sorption pressure–composition isotherms (PCI's) were obtained. The $La_{0.67}Ce_{0.19}Nd_{0.08}Pr_{0.06}Ni_5$ structural changes observed after annealing and discussed in Section 3.1 are correlated to the improvement in hydrogen sorption properties as shown in the PCI's curves of Figs. 4 and 5. Fig. 4 shows hydrogen absorption and desorption PCI's at different temperatures of the sample after the thermal treatment at 400 °C. This sample shows, unlike the as-milled one, a more defined plateau and an increment in the experimental capacity. A quantification of results is presented in Table 3.

As observed in Fig. 3, the PCI of the as-milled AB_5 exhibits both an extension of the α-phase and a large slope. It could be inferred from this behavior the presence of a high density of strain and zones containing different hydrogen concentration [26] as well as a nonhomogeneous occupancy of the A-sites of the AB_5. Therefore, the hydrogen storage up to 4000 kPa remains lower than the theoretical maximum hydrogen concentration (H wt% = 1.4). As observed in Fig. 4, the plateau absorption pressures decrease with larger hydrogen storage values as annealing temperature increases. A summary of results is presented in Table 4. In this table, the plateaus are defined for PCI's zones which slope value is lower than 1×10^3 kPa/H wt%.

It is concluded that the annealing treatment needs stronger conditions to fit the intermetallic for hydrogen compression application.

Hydrogen absorption and desorption properties were obtained after thermal treatment at 600 °C. The PCI's at 25, 35, 50, 70 and 90 °C and its corresponding Van't Hoff diagram are shown in Fig. 5. As observed, the sample exhibits flat defined plateaus and larger capacity than those of samples annealed at 400 °C. These results are correlated to the improvement of the microstructural properties shown in Fig. 1 and Tables 1–3. A quantification of the hydrogen sorption properties is shown in Table 4. Those of $LaNi_5$ after the same treatment are presented in the same table. From these results, the changes in hydride enthalpy ΔH° and entropy ΔS° of formation were calculated. The obtained results are summarized in Table 5 along with the ones of $LaNi_5$ [17].

Table 5 – Hydrides enthalpies and entropies of formation.

Sample	Treatment	ΔH (kJ/mol H_2)	ΔS (kJ/K mol H_2)
$LaNi_5$ – absorption	Milled + annealed 600 °C	-25.3 ± 0.3	-0.100 ± 0.001
$LaNi_5$ – desorption		-26.5 ± 0.5	-0.094 ± 0.002
$La_{0.67}Ce_{0.19}Nd_{0.08}Pr_{0.06}Ni_5$ – absorption		-29.0 ± 1.0	-0.113 ± 0.003
$La_{0.67}Ce_{0.19}Nd_{0.08}Pr_{0.06}Ni_5$ – desorption		-28.4 ± 0.8	-0.102 ± 0.002

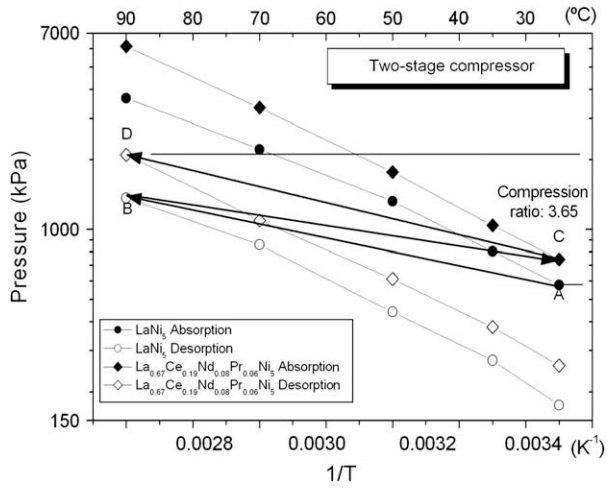

Fig. 6 – Two-stage thermal hydrogen compressor.

3.4. *Two-stage hydrogen compressor*

The Van't Hoff diagrams of $La_{0.67}Ce_{0.19}Nd_{0.08}Pr_{0.06}Ni_5$ and $LaNi_5$ [17] are shown in Fig. 6. Both intermetallics were synthesized by low energy mechanical alloying and thermally treated at 600 °C. From these results, a two-stage hydrogen compressor scheme was proposed. At the first stage, $LaNi_5$ absorbs hydrogen at 25 °C and 575 kPa (point A in Fig. 6). The system is isolated and heated at 90 °C. Hydrogen is desorbed at this temperature at 1365 kPa (point B). Then, hydrogen flows to the second stage containing $La_{0.67}Ce_{0.19}Nd_{0.08}Pr_{0.06}Ni_5$ which absorbs hydrogen at 25 °C and 745 kPa (C). After isolation and heating the system desorbs it at 90 °C and 2100 kPa (D). As a result, a compression ratio of 3.65 was achieved.

It is important to notice that eventual changes in the equilibrium pressures due to cycling will not affect the link between the stages because of the difference in the values of the desorption pressure of the first stage (1365 kPa) and absorption pressure of the second stage (745 kPa).

4. Conclusions

In this work, $La_{0.67}Ce_{0.19}Nd_{0.08}Pr_{0.06}Ni_5$ was synthesized by low energy mechanical alloying. Sample milling was stopped at *completion stage* in order to assure the achievement of final composition and an appropriate particle size distribution [11]. Structural and hydrogen sorption properties were analyzed and improved by annealing at $T = 600$ °C and $t = 24$ h. Both set of properties were quantified and compared to those of $LaNi_5$ obtained previously using the same synthesis-pretreatment method [17]. From the results obtained, thermodynamic data was calculated and a two-stage thermal compression of hydrogen was proposed. Hydrogen is compressed from 575 kPa (25 °C) to 1365 kPa (90 °C) using $LaNi_5$ as a hydride forming step. The fluid is supplied to a second stage where hydrogen is compressed from 745 kPa (25 °C) to 2100 kPa (90 °C) using $La_{0.67}Ce_{0.19}Nd_{0.08}Pr_{0.06}Ni_5$ as hydride forming material. The proposed scheme reaches a global 3.65 compression ratio. A third compression stage is the subject of an incoming work.

Acknowledgements

The authors wish to thank to the Agencia Nacional de Promoción Científica y Tecnológica of Argentina (Project 33473 and Project 12-15065), to the Consejo Nacional de Investigaciones Científicas y Técnicas of Argentina (Project PIP 6448) and to the Universidad Nacional de Cuyo of Argentina (Project 06/C256) for partial financial support.

REFERENCES

[1] Van Vucht JHN, Kuijpers FA, Bruning HC. Reversible room temperature absorption of large quantities of hydrogen by intermetallic compounds. Philips Res Rep 1970;25:133.
[2] Huston EL, Sandrock GD. Engineering properties of metal hydrides. J Less Comm Met 1980;72(2):435–43.
[3] Sandrock G. A panoramic overview of hydrogen storage alloys from a gas reaction point of view. J Alloys Compd 1999; 293–295:877–88.
[4] Kim JK, Park S, Kim KJ, Gawlik K. A hydrogen-compression system using porous metal hydride pellets of $LaNi_{5-x}Al_x$. Int J Hydrogen Energy 2008;33(2):870–7.
[5] Wang XH, Bei YY, Song XC, Fang GH, Li SQ, Chen CP, et al. Investigation on high-pressure metal hydride hydrogen compressors. Int J Hydrogen Energy 2007;32(16):4011–5.
[6] Dehouche Z, Savard M, Laurencelle F, Goyette J. Ti–V–Mn based alloys for hydrogen compression system. J Alloys Compd 2005;400(1–2):276–80.
[7] Dehouche Z, Grimard N, Laurencelle F, Goyette J, Bose TK. Hydride alloys properties for hydrogen sorption compressor. J Alloys Compd 2005;399(1–2):224–36.
[8] Laurencelle F, Dehouche Z, Goyette J, Bose TK. Integrated electrolyser-metal hydride compression system. Int J Hydrogen Energy 2006;31(6):762–8.
[9] Kai T, Uemura Y, Takanashi H, Tsutsui T, Takahashi T, Matsumoto Y, et al. A demonstration project of the hydrogen station located on Yakushima Island – operation and analysis of the station. Int J Hydrogen Energy 2007;32(15): 3519–25.
[10] Liang G, Huot J, Schultz R. Hydrogen storage properties of the mechanically alloyed $LaNi_5$-based materials. J Alloys Compd 2001;320(1):133–9.
[11] Esquivel MR, Andrade Gamboa JJ, Gennari FC, Meyer G. Synthesis of $MmNi_5$ by combined mechanical alloying low temperature heating process. In: Sohn international symposium advanced processing of metals and materials, vol. 4; 2006. p. 282–85.
[12] Esquivel MR, Meyer G. A comparison of the evolution during the mechanical alloying of both a $MmNi_5$–Ni and Mm–Ni mixtures: stages of milling and microstructural characterization. J Alloys Compd 2007;446–447:212–7.
[13] Singh A, Singh BK, Davidson DJ, Sristava ON. Studies on improvement of hydrogen storage capacity of AB_5 type: $MmNi_{4.6}Fe_{0.4}$ alloy. Int J Hydrogen Energy 2004;29(11):1151–6.
[14] Young RA, Larson AC, Paiva Santos CO. DBWS 9411, an upgrade of the DBWS programs for Rietveld refinement with PC and mainframe computers. J Appl Cryst 1995;28:366–7.
[15] Enzo S, Bonnetti E, Soletta I, Cocco G. Structural changes induced by the mechanical alloying of crystalline metal powders. J Phys D Appl Phys 1991;24:209–16.
[16] Meyer G, Rodriguez D, Castro F, Fernández G. Automatic device for precise characterization of hydride-forming materials. Hydrogen energy process. In: Proceedings of the 11th world hydrogen energy conference, vol. 2; 1996. p. 1293–298.

[17] Talagañis BA, Esquivel MR, Meyer G. Correlación entre las propiedades estructurales y de hidruración de aleaciones AB_5 should be subscript sintetizadas por molienda reactiva aplicables a compresión de hidrógeno. Anales AFA 2008;19: 206–10.
[18] Joint Committee for Powder Diffraction Standards. Powder diffraction file. Swarthmore, PA: International Center for Diffraction Data; 1996. card number 50-777.
[19] Massalski TB, editor. Binary alloy phase diagrams. Metals Park, Ohio: American Society for Metals; 1988. p. 1468.
[20] Joint Committee for Powder Diffraction Standards. Powder diffraction file. Swarthmore, PA: International Center for Diffraction Data; 1996. card number 51-1165.
[21] Joint Committee for Powder Diffraction Standards. Powder diffraction file. Swarthmore, PA: International Center for Diffraction Data; 1996. card number 87-0712.
[22] Joint Committee for Powder Diffraction Standards. Powder diffraction file. Swarthmore, PA: International Center for Diffraction Data; 1996. card number 36-1481.
[23] Joint Committee for Powder Diffraction Standards. Powder diffraction file. Swarthmore, PA: International Center for Diffraction Data; 1996. card number 13-0436.
[24] Mendelsohn MH, Gruen DM, Dwight AE. $LaNi_{5-x}Al_x$ is a versatile alloy system for metal hydride applications. Nature 1977;269:45–7.
[25] Senoh H, Takeichi N, Kiyobayashi T, Tanaka H, Takeshita HT, Oishi T, et al. Studies on P–C isotherms in RNi_5–H (R: La, Pr, Nd, Sm, Gd, Tb and Dy) systems. J Alloys Compd 2005;404–406:47–50.
[26] Iosub V, Latroche M, Joubert JM, Percheron-Guégan A. Optimisation of $MmNi_{5-x}Sn_x$ (Mm = La, Ce, Nd, Pr $0.27<x<0.5$) compositions as hydrogen storage materials. Int J Hydrogen Energy 2006;31:101–8.